Contents

1. Introduction 191
2. Observations 192
3. Theoretical Analysis 197
4. Conclusions 199
Acknowledgments 201
References 201

11. Analysis of Penumbral Eclipse Data

H. B. Garrett, 1/Lt. USAF
Air Force Geophysics Laboratory
Hanscom AFB
Bedford, Mass.

Abstract

Two days of data from the ATS-6 1976 eclipse season were analyzed to determine the effects of varying photoelectron flux on spacecraft potential. Particular emphasis was placed on the variation in potential as the satellite entered the earth's penumbra. Measurements from the AE-C satellite of the solar UV radiation were used to construct a model of atmospheric attenuation. This model was found to be consistent with direct measurements of the variations in photoelectron flux as INJUN V passed into eclipse. Applying the model to the ATS-6 data gave the time-dependency of the solar illumination/photoelectron flux as the satellite was eclipsed. This relationship, when combined with the ATS-6 measurements of satellite potential, revealed a nearly linear relation between the solar illumination/photoelectron flux and the logarithm of the satellite potential.

1. INTRODUCTION

The charging of spacecraft at geosynchronous orbit has become a primary concern for engineers and satellite designers. A major goal of scientists concerned with the problem is to provide to the engineers and designers adequate models of this phenomenon. Although several models of the sheath surrounding the spacecraft,

of the way in which this sheath alters the ambient particle fluxes, and of the subsequent interaction with the spacecraft surface exist in varying degrees of sophistication, few means exist for verifying these models.[1] The purpose of this report will be to present observations of the variation in the ATS-6 spacecraft potential as one parameter, the photoelectron flux, was varied in a known manner. This will be accomplished by detailed analysis of data from periods when the sun, as observed by a satellite, is eclipsed by the earth.

2. OBSERVATIONS

The highest potentials yet observed on spacecraft have been by the ATS-5 and ATS-6 satellites as they passed into the earth's shadow. These potentials are only observed when the satellites are immersed in the hot plasma associated with geomagnetic storms and plasma injection events. Briefly, as a satellite passes into eclipse, the incident solar photon flux is decreased resulting in a decrease in the photoelectron current emitted from the satellite surface. It is the elimination of this current source that results in a current imbalance which leads to a large negative potential.

Figures 1 and 2 are spectrograms for 28 February (Day 59) and 6 March (Day 66) of the particle populations observed by the ATS-6 satellite during the spring 1976 eclipse season (see[2] for an explanation of these spectrograms). The intense bands observed in each positive ion spectrogram are the cold background ion population which has been accelerated by electric fields on the spacecraft. These data can be interpreted as voltage changes on ATS-6 amounting to over -10,000 volts and are coincident with the passage of the satellite into eclipse. In Figure 3, the voltage changes as the spacecraft passes into eclipse (exits eclipse) are plotted as continuous (dashed) lines for Days 59 and 66. Entry and exit (reversed in time) have been superimposed on each other to show their agreement for each eclipse. This agreement is a consequence of the eclipse symmetry and the apparent stability of ambient conditions during each eclipse.

Figures 4 and 5 show the plasma distribution functions for the electrons and ions associated respectively with the eclipses on Day 59 and Day 66. Figure 4, for Day 59, shows the plasma conditions before and after eclipse (dashed lines) and during eclipse (solid lines). The spectra immediately before and after eclipse are nearly identical; whereas the spectra measured while the satellite was in eclipse show the effects of charging. Normally these effects result in a constant, positive

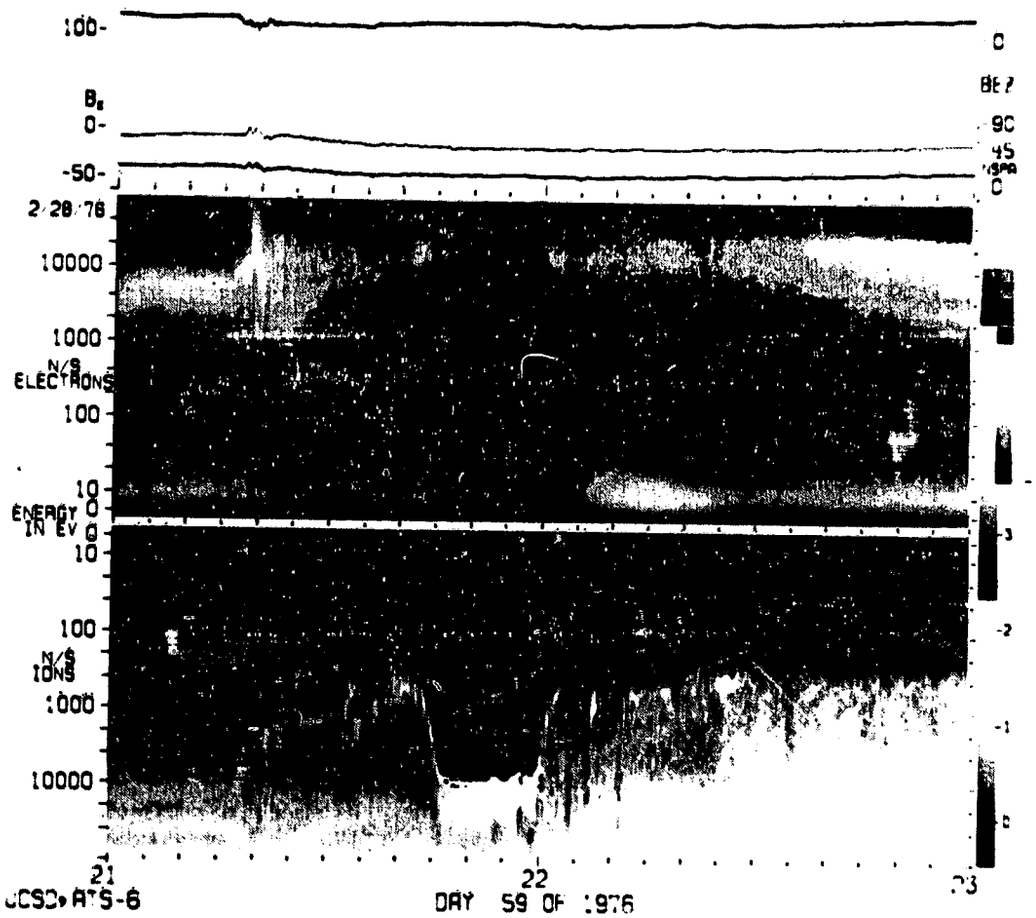

Figure 1. Spectrogram of ATS-6 Count Rates as a Function of Time and Energy for Day 59 of 1976. The spacecraft develops a potential of -10,000 V as reflected by the ion data when it is eclipsed near 2200 UT

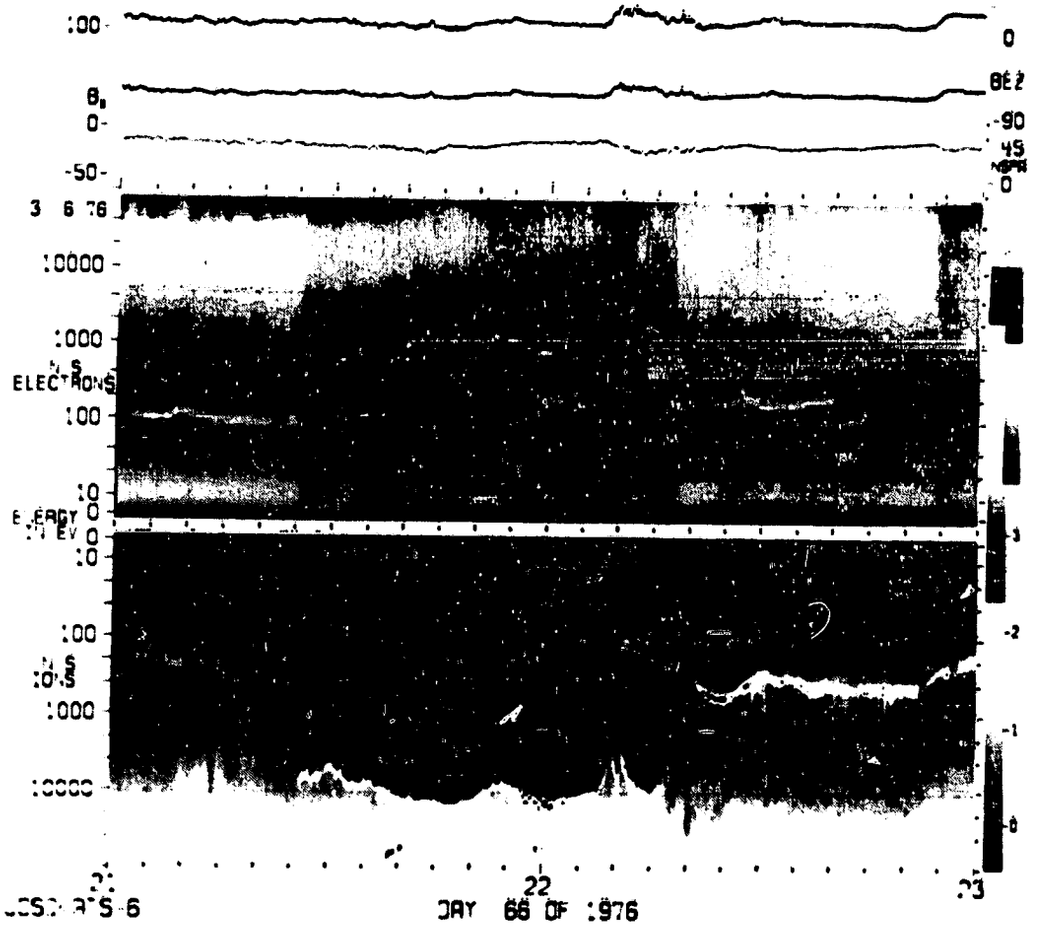

Figure 2. Spectrogram of ATS-6 Count Rates as a Function of Time and Energy for Day 66 of 1976. The spacecraft is eclipsed by the Earth between 2100 and 2300 UT

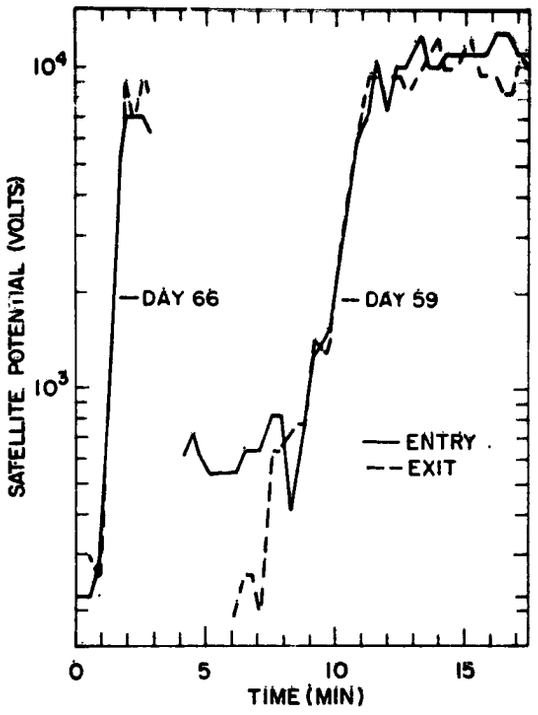

Figure 3. ATS-6 Potential as a Function of Time for Day 59 and Day 66. For reference, as the time axis is not absolute, ATS-6 had voltages in excess of -10,000 V for 1060 sec on Day 59 and 3126 sec on Day 66

displacement in energy of the ion distribution function that is equal to the potential on the satellite and a corresponding negative displacement in the electron distribution function. The spectra for Day 66 in Figure 6 show this effect, but, for energies above 30 keV, the spectra for Day 59 are not consistent with this behavior. The exact cause of the departure is not known but it may result from effects on the spacecraft due to the eclipse rather than to changes in the ambient plasma.

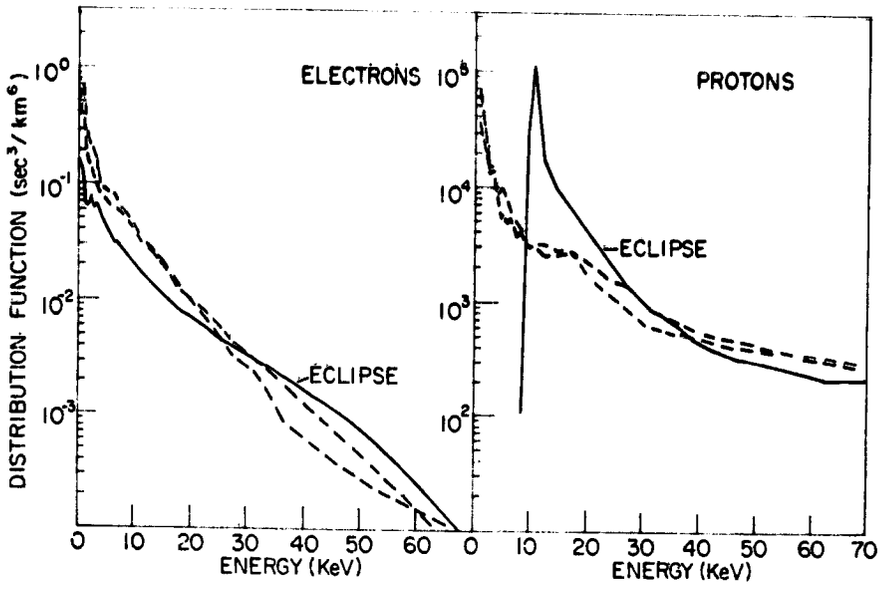

Figure 4. Electron and Ion Distribution Functions as Functions of Energy for Day 59. Dashed lines represent the spectra before and after eclipse. Solid lines represent eclipse spectra

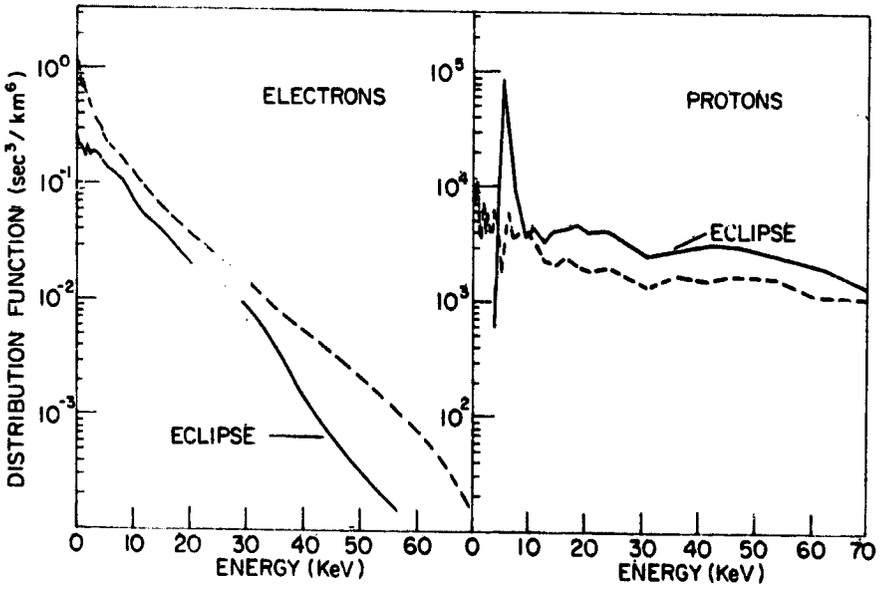

Figure 5. Electron and Ion Distribution Functions versus Energy for Day 66. Dashed lines represent spectra before eclipse. Solid lines represent eclipse spectra

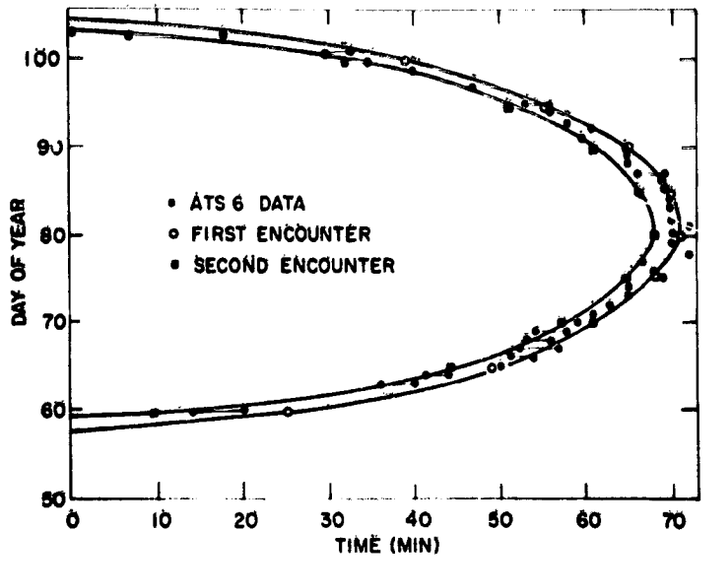

Figure 6. Duration of Penumbral and Umbral Eclipse Periods as a Function of Day of the Year for the ATS-6 1976 Spring Eclipse Season. Observed and predicted results are plotted

3. THEORETICAL ANALYSIS

In the preceding section, the experimental data were presented along with a brief description of the plasma conditions. Based on these data, I feel that the ambient plasma distribution during eclipse Days 59 and 66 did not change significantly except for a displacement in the distribution function due to charging effects. As previously discussed, it is the loss of the photoemission current as the sun is eclipsed which is the apparent source of the charging. To analyze the charging in more detail, it is necessary to accurately model the time variation of the solar illumination. To accomplish this, data from several sources will be used to compute and test a model of the penumbral variation.

A simple model of the penumbral region can be derived by assuming the earth and sun to be well defined discs. Geometry then gives a relation between the percentage of solar illumination and time. In Figure 6, the duration of eclipse versus day of year for the ATS-6 1976 spring eclipse season has been plotted. Where it was possible to estimate both, entry into the penumbral and umbral regions are shown connected by a line. The two curves represent the theoretical prediction of partial and total eclipse. The data indicate that even this simple theory gives an adequate prediction of the duration of partial and total eclipse at synchronous orbit. Note that Day 59 is an example of grazing incidence while Day 66 illustrates direct entry into eclipse.

The major objection to such a simple theory is the exclusion of atmospheric effects. For low altitudes (less than 2 earth radii), such effects are clearly important. This is demonstrated in Figure 7 where the variation of photoelectron flux (dots) versus time as the INJUN V satellite passed into eclipse is plotted. At the time of these data, the INJUN V satellite was at 1.5 earth radii. The solid line is a theoretical curve of the percentage of solar illumination versus time when atmospheric effects are included in the eclipse model. Ignoring atmospheric effects gives the dashed curve in Figure 7 (note: the earth's eclipse boundary was placed at 6378 km + 145 km for this calculation).

Using data from the AE-C satellite,[3] the attentuation, τ (such that $\phi = \phi_e e^{-\tau}$, where ϕ is the observed photon flux), as a function of minimum ray height above sea level, was calculated. At a given wavelength, it was readily found that:

$$\tau = e^{\frac{-(X - X_o)}{\delta}} \tag{1}$$

where

X = height above sea level,

X_o = constant, dependent on frequency of light, and

δ = scale height, dependent on frequency of light.

As the detailed variation of the photoelectron flux is dependent on the materials of which the spacecraft is constructed and as the atmosphere itself varies in time, it is difficult to construct a more exact model. Careful consideration of the photoelectron emission versus frequency and the attenuation versus frequency from the AE-C satellite gave average values of:

$$X_o = 145 \text{ km} \tag{2}$$

$$\delta = 23.5 \text{ km} \quad . \tag{3}$$

The INJUN V data of Figure 7 are fit with a value of 60 km for δ, whereas ATS-6 is better fit by $\delta = 23.5$ km. The difference is likely due to the materials of which the satellites are constructed as the INJUN V detector is made of tungsten which is responsive to longer wavelengths than aluminum, the primary ATS-6 material.

To first order, the effect of the atmosphere is to make the earth appear larger (approximately 145 km larger) in radius. Although δ is not accurately known, the AE-C data implies values of less than 100 km. This uncertainty generates timing errors in our estimation of the eclipse duration on the order of 30 sec or less but does not greatly alter the results to be presented. By comparison, emphemeris

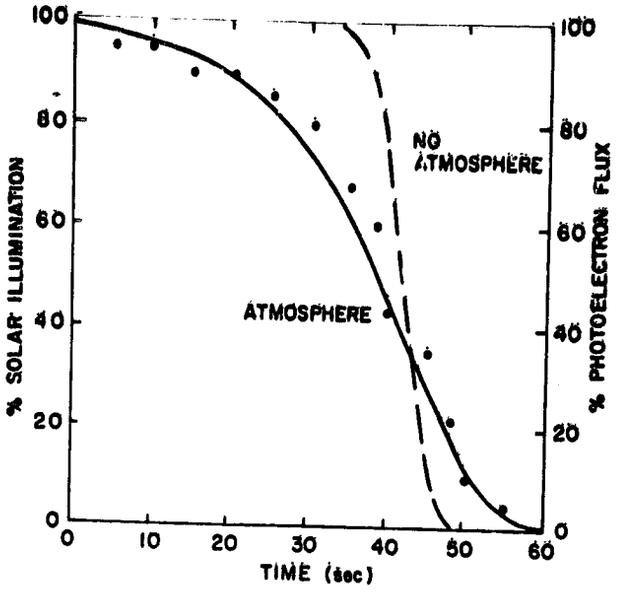

Figure 7. INJUN V Measurements of the Photoelectron Flux as a Function of Time in the Penumbral Region (Dots). Also shown are two theoretical curves of the solar illumination for the case of no atmosphere (dashed line) and with an atmosphere (solid line)

errors are of the same order indicating that the atmospheric model is consistent with the accuracy inherent in the problem.

4. CONCLUSIONS

The voltage data in Figure 3 can be fit as a function of time between roughly -2000 and -10,000 volts by:

$$\text{Day 59: } V \simeq -10^3 \, e^{0.016(T+530)} \tag{4}$$

$$\text{Day 66: } V \simeq -10^3 \, e^{0.05(T+1563)} \tag{5}$$

where V = voltage (volts)

T = time (seconds).

Assuming δ = 23.5 km and X_o = 145 km in the atmospheric model, the solar illumination versus voltage for Days 59 and 66 are plotted in Figure 8. The error bars are for the results arrived at by assuming no atmosphere (upper) or by assuming δ = 60 km (lower).

As the percentage of solar illumination is directly related to the photoelectron flux (Figure 7), Figure 8 can be interpreted as illustrating the effect of varying the photoelectron flux on the satellite potential. Timing errors in the ephemeris and the atmospheric model may alter the quantitative results of Figure 8 within roughly the error bars shown, but will not alter the qualitative result inherent in the figure -- namely that the voltage is proportional to the exponential of the photoelectron flux. This result is of real value as it can be used as a test of the predictions of various theoretical models. In particular, it can be used to check the modeling of photoelectron variations. As it is almost impossible to distinguish secondary and back-scattered electrons from photoelectrons, the results have broader implications since they can be applied to testing any model which includes the effects of variable electron emission. This latter observation is particularly important when one recalls that standard sheath models imply a logarithmic, not exponential, relation between electron emission and voltage.

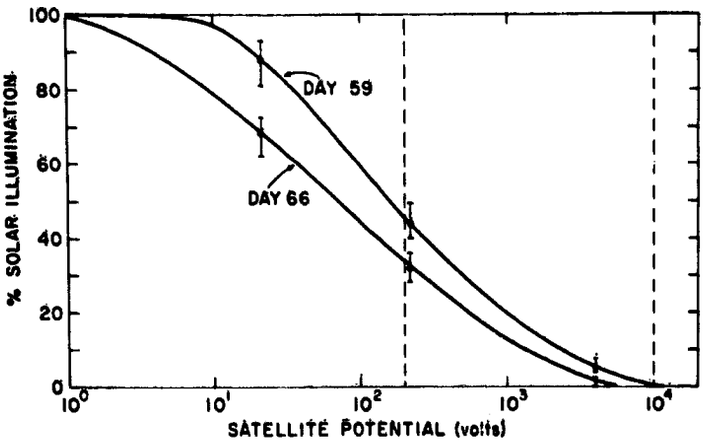

Figure 8. Composite Plot of the Solar Illumination (or Photoelectron Flux) as a Function of Satellite Potential for Day 59 and Day 66

Acknowledgments

I would like to thank Drs. DeForest and Whipple for providing the ATS-6 data and taking the time to explain data formats. Useful discussions were held with Drs. Burke (INJUN V data), Hinteregger (AE-C data), Rubin, Rothwell, and Pike.

References

1. DeForest, S. E. (1972) Spacecraft charging at synchronous orbit, J. Geophys. Res. 77:651-659.
2. DeForest, S. E., and McIlwain, C. E. (1971) Plasma clouds in the magnetosphere, J. Geophys. Res. 76:3587-3611.
3. Hinteregger, H. E., Bedo, D. E., and Manson, J. E. (1973) The EUV spectrophotometer on Atmosphere Explorer, Rad. Sci. 8(No. 4):349-359.